ADVANCED FUNCTIONAL MATERIALS
www.afm-journal.de

A Fluorophore-Doped Polymer Nanomaterial for Referenced Imaging of pH and Temperature with Sub-Micrometer Resolution

Xu-dong Wang, Robert J. Meier, and Otto S. Wolfbeis**

A new kind of pH and temperature sensitive material is reported. It is composed of dye-doped polymer nanoparticles incorporated into a thin film of a polyurethane hydrogel. The new pH/temperature-sensitive nanoparticles are obtained by post-staining oxygen-impermeable amino-functionalized polyacrylonitrile nanoparticles with a long-lifetime reference dye. Staining is followed by covalently linking fluorescein isothiocyanate onto the surface of the nanoparticle. The new sensor material has several distinct features: a) it enables imaging of pH via time domain dual-lifetime referencing; b) effects of temperature on pH sensing may be compensated for; and c) temperature can simultaneously be visualized via rapid lifetime imaging. The new material enables referenced and temperature-compensated pH imaging with superior spatial resolution due to the use of nanosized sensor nanoparticles.

1. Introduction

The determination of pH provides essential information for biology research,[1,2] medical treatment,[3] marine science,[4] environmental science,[5] pollution control,[6] food industry,[7] and agriculture.[8] The most convenient way to measure pH, of course, is based on the use of pH electrodes. Further, colorimetric pH test strips with either visual or instrumental read-out are in widespread use. These two methods offer varying analytical ranges and precisions for different fields of applications. The pH electrodes are precise and enable continuous measurement using small and affordable instrumentation. On the other side, they are difficult to miniaturize, require two-point calibration, are sensitive to electrical fields, difficult to use in remote sensing, need a reference electrode, can be interfered by heavy metal ions, and only allow for single-spot measurements. Colorimetric test strips are less precise (unless quantitatively read out via reflectometers), but versatile and easy to operate. More precise approaches have been described where luminescence based pH sensor strips are being read out with instrumentation such as CCD cameras.[9–11] Recently, the use of digital cameras for optical pH read-out also has been reported.[12,13] Optical pH sensors can be miniaturized down to the micrometer scale (for example in the form of fiber optics)[14] and even nanometer scale (in the form of nanoparticles). The latter even enables intracellular sensing of pH. [1,15,16]

Optical pH sensors, in contrast to electrodes, usually respond over a limited analytical range only. However, they have the particular feature of enabling the two-dimensional distribution of pH to be imaged if deposited in planar form, typically as a thin film. Most optical methods are based on fluorescence, which - unlike absorption - can be easily detected from top. This is needed in case of strongly colored or bulky objects such as tissue or other biomaterial.[3,12] Fluorescence intensity based imaging techniques need referencing in most cases. The measurement of luminescence lifetime (as opposed to intensity) is particularly attractive because it is virtually a referenced method that is insensitive to signal drifts caused by fluctuation of the intensity of the light source, by probe concentration and photobleaching, by variations in the distance between sensor layer and detector, and by background light and ambient light. This is due to the fact that luminescence lifetime is an intrinsic property of any fluorophore that can be determined fairly easily. Luminescent lifetime represents a self-referenced signal that does not suffer from the limitations discussed above.

We are presenting here a new kind of material that has the specific merits of enabling imaging of pH with very high spatial resolution because it is making use of nanoparticles to which a pH indicator dye is covalently linked. In addition, the nanoparticles are doped with a long-lived reference luminophore so that the information on pH can be read out by the time domain dual-lifetime referencing (td-DLR) method,[17] which makes the system particularly robust in terms of accuracy. More over, the decay time of the reference dye strongly depends on temperature, and this is used to sense and to image this parameter.

2. Results and Discussions

2.1. Probes and Materials

The material used is composed, in essence, of nanoparticles made from polyacrylonitrile (PAN) that are incorporated into a

Dr. X.-d. Wang, Dr. R. J. Meier, Prof. O. S. Wolfbeis
Institute of Analytical Chemistry
Chemo- and Biosensors
University of Regensburg
D-93040 Regensburg, Germany
E-mail: xmuwxd@gmail.com;
otto.wolfbeis@chemie.uni-r.de

DOI: 10.1002/adfm.201200813

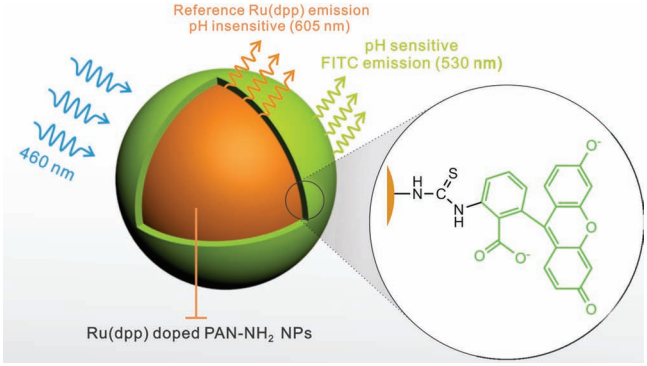

Figure 1. The core-shell structure of Ru(dpp)-doped PAN-FITC nanoparticles.

layer of polyurethane hydrogel. The nanoparticles were doped with the reference dye tris(4,7-diphenyl-1,10-phenanthroline) ruthenium(II) trimethylsilyl[18] (referred to as Ru(dpp)), as shown in orange color in **Figure 1**, by the well-developed post-swelling and -staining approach.[19] The surface of the nanoparticles contains reactive amino groups. These can be used for covalently linking the pH responsive probe fluorescein isothiocyanate (FITC) to the particle surface. A pH sensitive shell is generated, as depicted in green color in Figure 1. The resulting nanoparticles are referred to as Ru(dpp)-doped PAN-FITC nanoparticles. If excited at 460 nm using a blue LED, the nanoparticles emit a) a pH-dependent green emission with a maximum at 530 nm and b) a pH-insensitive orange emission peaking at 605 nm. Most notable, the absorption and emission spectra of the dyes used are such that fluorescence resonance energy transfer (FRET) cannot occur despite their spatial proximity. The pH probe is located at the surface of the nanoparticles and thus exposed to the aqueous sample. This is beneficial in terms of rapid equilibration.

2.2. Optical Readout

Two fluorometric methods for signal readout are being used here. The first is time domain dual lifetime referencing (td-DLR), and the second is rapid lifetime determination (RLD). Lifetime based imaging is a highly useful method in fluorometry because it enables self-referenced (more robust) sensing. However, most luminescent pH probes exhibit lifetimes that are too short (in the ns range) for affordable lifetime imaging systems that do not use microscopic scanning.[20] The instrumental effort to measure such short lifetimes is unnecessarily complex compared to the ease of determining lifetimes in the order of microseconds or milliseconds. Long-lifetime based sensing and imaging of pH values can be based on either a) the use of long-decaying pH probes[21–23] or b) by making use of dual-lifetime referencing (DLR). In the latter scheme (used here), a reference dye (or dyed nanoparticles) are added to a ns-decaying pH probe. The two dyes have spectral properties that strongly overlap. In DLR, the pH-dependent changes in the risetime and the decay time of the total luminescence, or the pH-induced phase shifts of sinusoidally modulated light are determined. In other words: the DLR method can be operated in either the time-domain (td) mode[3,4,24,25] or the frequency-domain (fd) mode.[8,26–30] Discovered in 2001, it enables both sensing and imaging short-lived luminescence.[2,3,17–23] Instrumentation for performing td-DLR is affordable and small.

The principle of td-DLR is schematically shown in **Figure 2**. In essence, the luminescence of the short-lived indicator (shown in green) and of the long-lived reference dye Ru(dpp) (shown in orange) are simultaneously excited and measured in two time gates (A_1 and A_2). The first gate (A_1) records the intensity of light during the excitation period (light source switched on). This signal is composed of short-lived fluorescence and long-lived luminescence. The second gate (A_2) is recorded during the emission period in which the short-lived pH dependent signal is already decayed. The intensity of A_2 is exclusively composed of the reference luminescence. Rationing of the images recorded in gates A_1 and A_2 results in an intrinsically referenced pH dependent signal.

In addition, one can record the area of gate A_3. Combined with the signal of gate A_2, the lifetime of the reference dye Ru(dpp) can be measured via the rapid lifetime determination (RLD) method.[31,32] There is a relationship between the lifetime of Ru(dpp) and temperature which therefore also can be used to calculate temperature. Its knowledge also enables internal temperature compensation which is obligatory since the signals of the pH probe are affected by temperature.[33]

2.3. The Need to Use Particles

The accuracy and spatial resolution of td-DLR based imaging strongly depends on the spatial proximity and a constant ratio of pH-sensitive probe and the reference dye.[25] Practically all current td-DLR-based methods are utilizing fluorophores (the

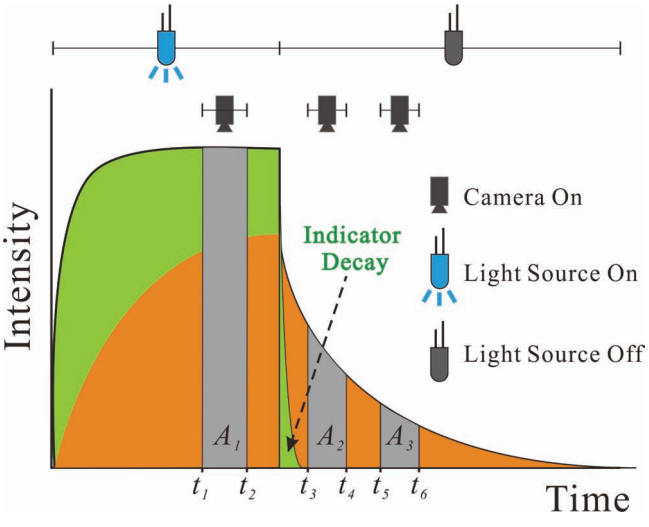

Figure 2. Schematic of the methods used for optical read-out. The time gates A_1 to A_3 can be use for td-DLR (to yield fluorescence lifetime-images for pH sensing) and for rapid lifetime determination (RLD; to yield information on temperature).

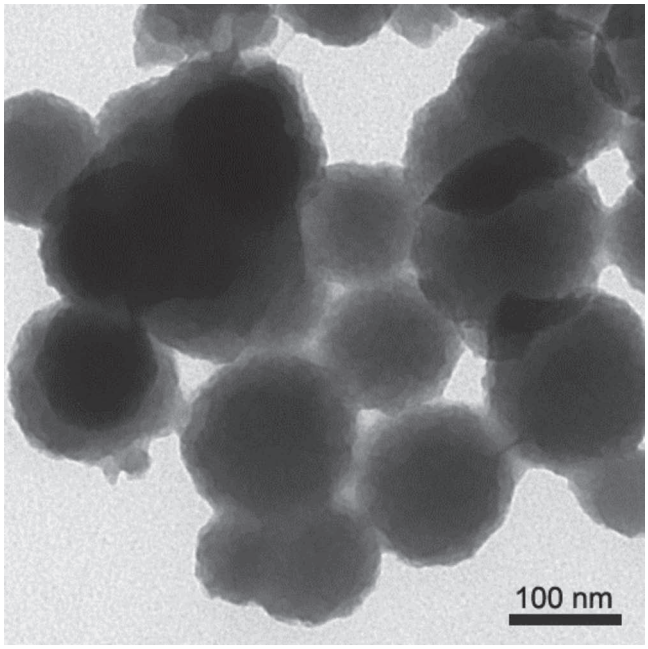

Figure 3. Transmission electron microscopy image of Ru(dpp)-doped PAN-FITC nanoparticles.

probe and the references dye) incorporated into spatially separated microparticles[3,34,35] (as shown in Figure 4, sensing film 1). In case of imaging pH, the probes usually are covalently immobilized in a highly proton-permeable matrix such as microparticles of aminoethyl-cellulose, while the long-lifetime reference dye usually is encapsulated in microparticles made from an oxygen-impermeable polymer (such as polyacrylonitrile) so to prevent oxygen to interfere by acting as a quencher. The use of microparticles prevents the occurrence of FRET between two fluorophores, and works quite well in case of thick sensor films and if low imaging resolution is adequate. If, however, high resolution is desired, the random distributions of the microparticles is causing local inhomogeneities which - in turn - can induce inaccuracies.

Figure 3 shows a transmission electron microscopic image of the fluorescence labeled pH responsive nanoparticles doped with Ru(dpp). They have a mean diameter of 150 nm and are virtually monodisperse. Such nanoparticles were expected to enable high resolution imaging, can be hardly applied to the surface of interest such as skin or other tissue, or to analytical Microsystems. One preferred way to generate homogeneously thin sensing films is to immobilize the nanoparticles in a layer of a polyurethane hydrogel.

2.4. Sensor Films and Imaging of pH

The sensor films were prepared from a cocktail composed of a solvent and the hydrogel (a highly transparent and biocompatible polyurethane) to which the (insoluble) nanoparticles are added as described in the Experimental Section. This cocktail is deposited on the surface of interest (or on plastic or glass) in appropriate thickness, and the solvent is evaporated. Typical thicknesses range from 0.5 to 15 µm, the lower limit being dependent on the size of the sensor particles.

In order to demonstrate the differences in the design of former sensor films and the new one presented here, a cross section is given in **Figure 4**. Conventional sensing films (#1) have large particles (2–5 µm thick) that do not enable thinner films to be made. In addition, the probe and the reference dye are incorporated into two different kinds of host material. The new type of sensing film (#2), in contrast, consists of much smaller (≈150 nm) particles of one kind only that do contain both dyes.

Sensing film 2, unlike film 1, is displaying high uniform pH distribution and excellent spatial resolution. If two kinds of particles are used, they will be randomly distributed as shown in the microscopic picture (Figure 4, sensing film 1). They show local variations in terms of dye concentration, in the worst case with regions with no pH sensitive microparticles, and this can result in erroneous data. In the new material and sensor film presented here (sensing film 2 in Figure 4), the pH sensitive probe and the reference dyes are contained in the same nanoparticles. Therefore, the pH-dependent (green) signal and the (red) reference signal are emitted at the same site, thus, leading to very homogenous signal distribution. The orange fluorescence of the sensor films at pH 3, and their more greenish fluorescence at pH 8 are the result of the varying contributions of the green and the orange emissions from the two fluorophores as a function of pH.

Figure 5A gives a time trace of the intensities of the green emission (plot (a)), the red emission (plot (b)), and their ratio (plot (c)). The green emission (a) gradually increases with increasing pH from 3 to 8, while the

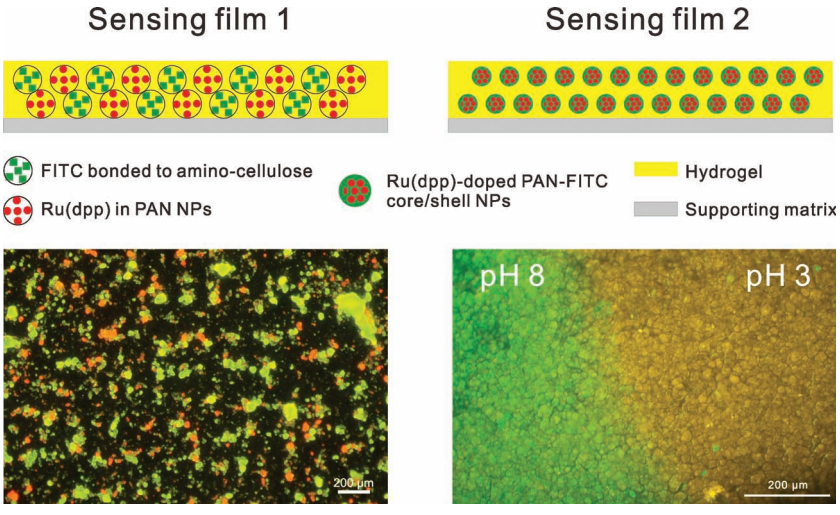

Figure 4. Schemes (top) of a conventional sensing film 1 using two spatially separated kinds of microparticles (referencing and pH sensing), and the current sensing film 2 using the Ru(dpp)-doped PAN-FITC nanoparticles; the bottom row depicts fluorescence microscopic images of sensing films 1 and 2, respectively.

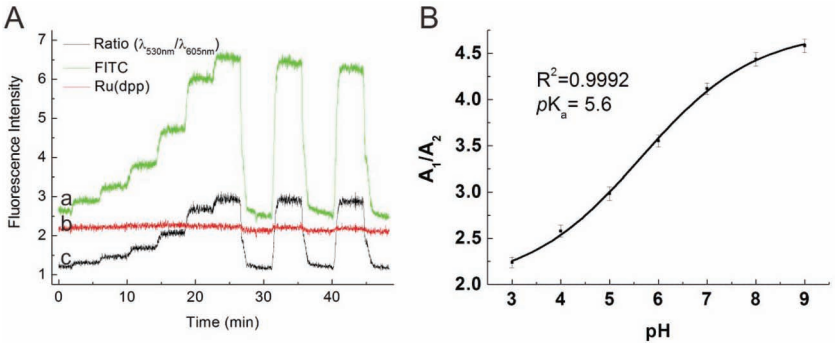

Figure 5. A) pH responses of the Ru(dpp)-doped PAN-FITC nanoparticles. Plot (a): the pH response of FITC emission; plot (b): the pH response of the reference dye Ru(dpp) emission; and plot (c): the ratio between the green FITC emission and Ru(dpp) emission at different pH. B) The pH response calibration curve based on td_DLR measurement.

orange luminescence of the reference dye Ru(dpp) remains constant. On forming the ratio between the pH responsive emission at 530 nm and the reference emission at 605 nm, the signal drift caused by light source fluctuation and other system errors is eliminated (plot c). It is also obvious that the new sensor material offers a fast response to pH changes (2–3 min) without hysteresis and further, a good reversibility. Figure 5B gives a calibration plot of the td-DLR signal (A_1/A_2) versus pH. It reveals sigmoidal response and small error bars.

As in case of many other triplet emitters with long lifetime, the luminescence intensity and lifetime of the long-lived reference dye Ru(dpp) may be quenched by oxygen which would represent a highly undesired side effect. The effect of oxygen on the luminescence of Ru(dpp) in the PAN-FITC nanoparticles is given in Figure S1 (Supporting Information) and shows that it has a negligible effect, obviously due to the gas-blocking properties of the PAN polymer used.[36] This property further warrants the shielding of other quenchers and the stability of the reference signal. The pK_a value of the sensor film is 5.6 at 22 °C and the dynamic range is from pH 4–9, which makes it suitable for biological applications. It shall be reminded here that optical sensors suffer from cross interferences by the ionic strength of the sample solution.[37] Both dyes on the nanoparticles suffer from slight photobleaching (as shown in Figure S2, Supporting Information). However, the ratio between the two emissions becomes much more stable, and undergoes a photodecomposition of 3.2% only per hour. The use of pulsed excitation in the td-DLR method will further diminish this.

In order to prove its high-resolution imaging capabilities, the sensor film was examined by lifetime fluorescence microscopy. The sensing film 2 was soaked in pH 3.0 buffer solution, blotted and subsequently covered with a tiny droplet of pH 8.0 buffer solution. The sensing area was visualized via the td-DLR method. As shown in **Figure 6** the pH value at the drop position is distinctly different from that of the residual area. The pH distributions in these two distinct regions are virtually uniform, and even the pH gradient in the boundary zone is precisely imaged. All these findings are proof that the new sensing film can be used for pH-imaging with sub-micrometer resolution.

2.5. Cross-Sensitivity Towards Temperature, and Imaging of Temperature

All known chemical sensors suffer from effects caused by temperature (T). Therefore, it is highly desirable (if not mandatory) to know the actual T at the site of sensing. The material presented here offers a particular feature in that the decay time of the reference fluorophore Ru(dpp) strongly depends on T.[17,38] **Figure 7**A reveals the linear relationship between T and the lifetime as determined by the RLD method.[17] Measurements at different oxygen partial pressures also revealed that the sensor signal is independent of oxygen tension. The determination of T via RLD allows for compensation of the effect of T on pH signal.

In addition to compensation, the homogenous distribution of the nanoparticles in the sensor film may even be used for imaging T as shown in Figure 7B. The sensor film reveals a homogenous distribution of T at either 50, 25, and 5 °C. This unique feature makes the new Ru(dpp)-doped PAN-FITC nanoparticles in the polyurethane sensing film a most useful material for simultaneously sensing and imaging of pH and temperature.

3. Conclusion and Perspectives

We have synthesized Ru(dpp)-doped PAN-FITC nanoparticles that enable imaging of pH. Their preparation is very straightforward and based on a post-staining approach. The nanoparticles are mono-dispersed and have a diameter of around 150 nm. The pH-sensitive fluorescence and the reference signal are emitted by the same nanoparticles. This results in high

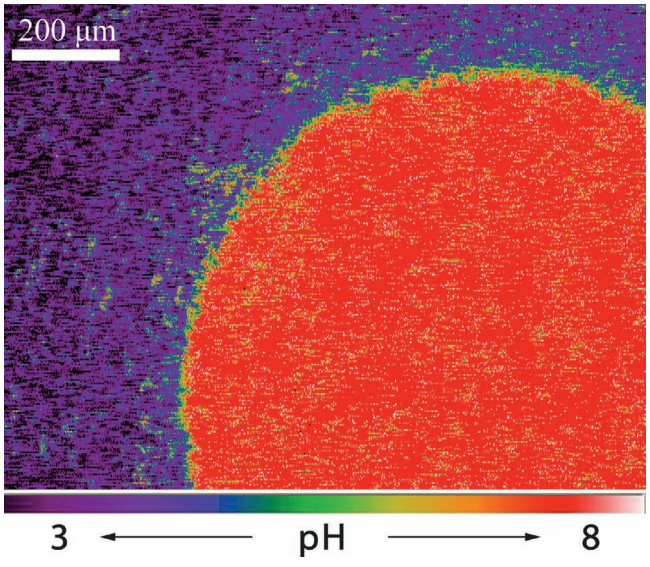

Figure 6. Microscopic td-DLR pH image of a drop of pH 8.0 buffer solution on a high-resolution pH sensor film.

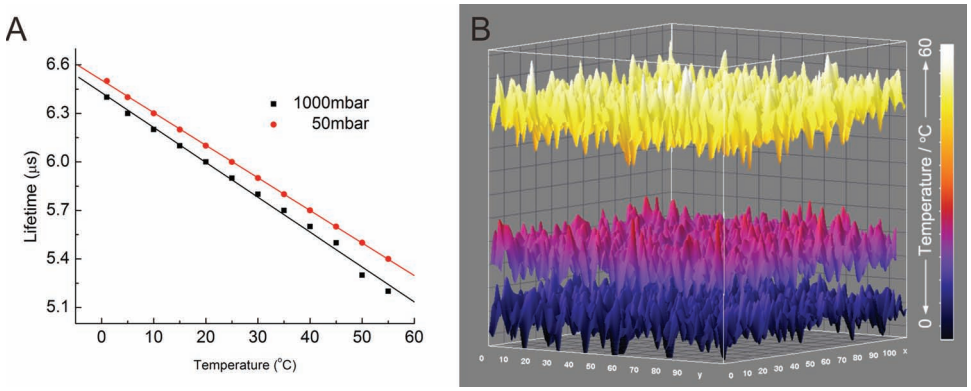

Figure 7. A) Relationship between temperature and lifetime of the reference dye Ru(dpp) inside the sensing film 2 measured using the RLD method. B) Temperature imaging based on RLD method.

spatial resolution imaging of pH. The ruthenium dye has a long lifetime that decreases with increasing temperature, and this enables temperature to be imaged, again with high spatial resolution. The scheme for dual sensing and imaging presented here may find applications in high-resolution sensing of pH (and its changes over time) and of temperature in micro- and nanofluidic systems[39,40] in micro-, nano-, and femtovolume (bio)chemistry,[41] or where exothermal chemical reactions[42] or enzymatic reactions[43] occur on a micro- or nanoscale.

4. Experimental Section

Preparation of the Ru(dpp)-Doped PAN-FITC Nanoparticles: Typically, amino-functionalized polyacrylonitrile nanoparticles (200 mg, referred as PAN-NH_2, from OptoSense GmbH; www.presens.de Germany) were dispersed in a mixture of distilled water (20 mL) and tetrahydrofuran (4 mL, THF). Subsequently, Ru(dpp) in THF (4 mL, 1 mg/mL) were slowly added under ultrasonic treatment. Ultrasonication was continued for 20 min, and the resulting Ru(dpp)-doped PAN-NH_2 nanoparticles were centrifuged and washed using water and ethanol (5 times each).

Fluorescein isothiocyanate (FITC) was then covalently attached to the surface of nanoparticles. Typically, Ru(dpp)-doped PAN-NH_2 nanoparticles (100 mg) were dispersed in a Britton-Robinson buffer solution (20 mL, 30 mM, pH 9.0), followed by addition of FITC in methanol (1.0 mL, 0.25 mg/mL). The solution was shaken over night. The Ru(dpp)-doped PAN-FITC nanoparticles thus obtained were shortly washed with 1.0 mM NaOH (twice), 1.0 mM HCl (twice), distilled water (8 times) and ethanol (4 times) in order to remove unreacted and adsorbed dyes. The nanoparticles obtained were then dispersed in a 5.0% (w/v) solution of a polyurethane hydrogel (type D4; from Cardiotech, www.advbiomaterials.com) in 90% (w/w) ethanol in water resulting in a "cocktail" with particles in a final concentration of 25 mg/mL.

Preparation of the Sensing Films: Sensing film 1 was prepared according to the literature.[3] Sensing film 2 was prepared by knife-coating the above cocktail on a polyester foil (Mylar; Goodfellow, UK; www.goodfellow.com). The solution was dried at room temperature to result in a sensing film with a thickness of 3 µm. The sensor films were stored in darkness at room temperature to prolong the shelf time.

Characterization of the Sensor Films: Fluorescence microscopic images were recorded on an inverted epifluorescence microscope (Nikon; www.nikon.com) equipped with a mercury arc lamp, an excitation bandwidth filter (420 to 490 nm), a 500-nm dichroic mirror and a long-pass filter for emission wavelengths of >520 nm. pH imaging via td-DLR was conducted by means of an ImageX Time Gated Imaging system (TGI; Photonic Research Systems; www.prsbio.com) with an integrated 12-bit CCD chip (640 × 480 pixels). The system was combined with a 460-nm LED for excitation. Parameters were set as follows: 9 µs gate width, 0.25 µs delay time, 10 µs lamp pulse, and 200 ms integration time. Temperature imaging based on the RLD method was performed with a PCO SensiCam 12 bit b/w CCD camera (PCO, Kelheim, Germany) and a 460-nm LED for excitation. The parameters for the RLD method were set as follows: 0.5 µs delay time, 3 µs gate width. The second gate was opened subsequently without delay.

Supporting Information

Supporting Information is available from the Wiley Online Library or from the author.

Acknowledgements

X.-d.W. and R.J.M. contributed equally to this work. This work was financially supported by the Alexander von Humboldt Foundation (Bonn) through a fellowship to X.-d.W. and the Deutsche Forschungsgemeinschaft DFG (SCHA1009/7-1), which are gratefully acknowledged.

Received: March 22, 2012
Revised: May 4, 2012
Published online: June 13, 2012

[1] J. Y. Han, K. Burgess, *Chem. Rev.* **2010**, *110*, 2709.
[2] A. S. Kocincová, S. Nagl, S. Arain, C. Krause, S. M. Borisov, M. Arnold, O. S. Wolfbeis, *Biotechnol. Bioeng.* **2008**, *100*, 430.
[3] S. Schreml, R. J. Meier, O. S. Wolfbeis, M. Landthaler, R.-M. Szeimies, P. Babilas, *Proc. Natl. Acad. Sci. USA* **2011**, *108*, 2432.
[4] C. R. Schroder, B. M. Weidgans, I. Klimant, *Analyst* **2005**, *130*, 907.
[5] F. Canete, A. Rios, M. D. L. de Castro, M. Valcarcel, *Analyst* **1987**, *112*, 263.
[6] K. Cammann, *Sens. Actuators, B* **1992**, *6*, 19.
[7] A. J. Marshall, J. Blyth, C. A. B. Davidson, C. R. Lowe, *Anal. Chem.* **2003**, *75*, 4423.
[8] V. Adamchuk, E. Lund, T. Reed, R. Ferguson, *Precis. Agric.* **2007**, *8*, 139.

[9] M. Hassan, J. Riley, V. Chernomordik, P. Smith, R. Pursley, S. B. Lee, J. Capala, A. H. Gandjbakhche, *Mol. Imaging* **2007**, *6*, 229.
[10] R. Niesner, B. Peker, P. Schlüsche, K.-H. Gericke, C. Hoffmann, D. Hahne, C. Müller-Goymann, *Pharm. Res.* **2005**, *22*, 1079.
[11] K. M. Hanson, M. J. Behne, N. P. Barry, T. M. Mauro, E. Gratton, R. M. Clegg, *Biophys. J.* **2002**, *83*, 1682.
[12] R. J. Meier, S. Schreml, X. D. Wang, M. Landthaler, P. Babilas, O. S. Wolfbeis, *Angew. Chem. Int. Ed.* **2011**, *50*, 10893.
[13] H. X. Chen, X. D. Wang, X. H. Song, T. Y. Zhou, Y. Q. Jiang, X. Chen, *Sens. Actuators, B* **2010**, *146*, 278.
[14] L. Jie, *TrAC, Trends Anal. Chem.* **2000**, *19*, 541.
[15] Y. E. K. Lee, R. Kopelman, *Methods Enzymol.* **2012**, *504*, 419.
[16] Y.-E. K. Lee, R. Kopelman, *Wiley Interdiscip. Rev. Nanomed. Nanobiotechnol.* **2009**, *1*, 98.
[17] G. Liebsch, I. Klimant, O. S. Wolfbeis, *Adv. Mater.* **1999**, *11*, 1296.
[18] I. Klimant, O. S. Wolfbeis, *Anal. Chem.* **1995**, *67*, 3160.
[19] X. D. Wang, H. H. Gorris, J. A. Stolwijk, R. J. Meier, D. B. M. Groegel, J. Wegener, O. S. Wolfbeis, *Chem. Sci.* **2011**, *2*, 901.
[20] C. W. Chang, D. Sud, M. A. Mycek, *Methods Cell Biol.* **2007**, *81*, 495.
[21] Y. Clarke, W. Xu, J. N. Demas, B. A. DeGraff, *Anal. Chem.* **2000**, *72*, 3468.
[22] Z. Murtaza, Q. Chang, G. Rao, H. Lin, J. R. Lakowicz, *Anal. Biochem.* **1997**, *247*, 216.
[23] N. B. Borchert, G. V. Ponomarev, J. P. Kerry, D. B. Papkovsky, *Anal. Chem.* **2010**, *83*, 18.
[24] T. Mayr, C. Igel, G. Liebsch, I. Klimant, O. S. Wolfbeis, *Anal. Chem.* **2003**, *75*, 4389.
[25] G. Liebsch, I. Klimant, C. Krause, O. S. Wolfbeis, *Anal. Chem.* **2001**, *73*, 4354.
[26] S. M. Borisov, K. Gatterer, I. Klimant, *Analyst* **2010**, *135*, 1711.
[27] K. Waich, S. Borisov, T. Mayr, I. Klimant, *Sens. Actuators, B* **2009**, *139*, 132.
[28] S. M. Borisov, G. Neurauter, C. Schroeder, I. Klimant, O. S. Wolfbeis, *Appl. Spectrosc.* **2006**, *60*, 1167.
[29] T. Mayr, I. Klimant, O. S. Wolfbeis, T. Werner, *Anal. Chim. Acta* **2002**, *462*, 1.
[30] C. Huber, I. Klimant, C. Krause, O. S. Wolfbeis, *Anal. Chem.* **2001**, *73*, 2097.
[31] R. B. Rexwinkel, P. Schakel, S. C. J. Meskers, H. P. J. M. Dekkers, *Appl. Spectrosc.* **1993**, *47*, 731.
[32] R. J. Woods, S. Scypinski, L. J. C. Love, H. A. Ashworth, *Anal. Chem.* **1984**, *56*, 1395.
[33] S. Nagl, O. S. Wolfbeis, *Analyst* **2007**, *132*, 507.
[34] M. I. J. Stich, M. Schaeferling, O. S. Wolfbeis, *Adv. Mater.* **2009**, *21*, 2216.
[35] G. S. Vasylevska, S. M. Borisov, C. Krause, O. S. Wolfbeis, *Chem. Mater.* **2006**, *18*, 4609.
[36] J. Comyn, *Polymer permeability*, Chapman & Hall, London **1985**.
[37] J. Janata, *Anal. Chem.* **1987**, *59*, 1351.
[38] L. H. Fischer, M. I. J. Stich, O. S. Wolfbeis, N. Tian, E. Holder, M. Schäferling, *Chem. Eur. J.* **2009**, *15*, 10857.
[39] T. Robinson, Y. Schaerli, R. Wootton, F. Hollfelder, C. Dunsby, G. Baldwin, M. Neil, P. French, A. deMello, *Lab Chip* **2009**, *9*, 3437.
[40] D. Ross, M. Gaitan, L. E. Locascio, *Anal. Chem.* **2001**, *73*, 4117.
[41] H. H. Gorris, D. R. Walt, *Angew. Chem. Int. Ed.* **2010**, *49*, 3880.
[42] A. J. deMello, *Nature* **2006**, *442*, 394.
[43] A. Huebner, L. F. Olguin, D. Bratton, G. Whyte, W. T. S. Huck, A. J. de Mello, J. B. Edel, C. Abell, F. Hollfelder, *Anal. Chem.* **2008**, *80*, 3890.